ICSO 2016

International Conference on Space Optics

Biarritz, France

18–21 October 2016

Edited by Bruno Cugny, Nikos Karafolas and Zoran Sodnik

Application of spinal code for performance improvement in free-space optical communications

Naoya Saiki

Eiji Okamoto

Hideki Takenaka

Morio Toyoshima

esa icso proceedings cnes

International Conference on Space Optics — ICSO 2016, edited by Bruno Cugny, Nikos Karafolas, Zoran Sodnik, Proc. of SPIE Vol. 10562, 105622Q · © 2016 ESA and CNES
CCC code: 0277-786X/17/$18 · doi: 10.1117/12.2296175

APPLICATION OF SPINAL CODE FOR PERFORMANCE IMPROVEMENT IN FREE-SPACE OPTICAL COMMUNICATIONS

Naoya Saiki[1], Eiji Okamoto[1], Hideki Takenaka[2], and Morio Toyoshima[2] .
[1]*Department of Electrical and Mechanical Engineering, Nagoya Institute of Technology*
Gokisocho, Showa-ku, Nagoya, 466-8555 Japan.
[2]*Space Communications Laboratory, Wireless Network Research Center,*
National Institute of Information and Communications Technology
4-2-1, Nukui-Kitamachi, Koganei, Tokyo, 184-8795 Japan.
E-mail: 28413077@stn.nitech.ac.jp

I. INTRODUCTION

In recent years, the demand for high-capacity communication has grown, and fiber-optic transmission is being used in wired communications to meet this demand. Similarly, free-space optics (FSO), which is an optical wireless communication technology that uses laser light, has attracted much attention and has been considered as a suitable alternative to satisfy this demand in wireless communications. Free-space optical communication uses a hundred THz frequency band and allows for high-speed and radio-regulation free transmission, which may provide a solution for the current shortage of radio frequency bands. In addition, laser transmission and radio wave transmission do not interfere with each other, and the sharp directivity of an optical wave can ensure secure communication. The optical devices can be compact because of high-frequency waves. The National Institute of Information and Communications Technology has successfully performed satellite-to-ground and inter-satellite laser communications experiments, and has developed various optical technologies for practical realization [1].

However, there are two major problems in free-space optical communications: optical scintillation and pointing error of the lens. When a laser beam passes through air, like in a satellite-to-ground link, optical scintillation occurs and the received optical power fluctuates. In addition, because of the sharp directivity of laser light, the pointing and tracking range between facing lenses becomes narrow, resulting in the frequent occurrence of pointing and tracking error, especially in mobile communications. These phenomena result in the reduction of received optical power. Because FSO usually aims at high-capacity transmission, burst erasure or burst error occurs in the laser channel even if the fade period is very short. Therefore, to realize high-capacity and high-quality laser transmission, measures for reducing burst error are indispensable.

Channel coding is used as a general scheme for reducing error. Channel coding consists of automatic repeat request (ARQ) and forward error correction (FEC), and an integrated use of both is the most effective. However, the distance between a satellite and an earth station, or between two satellites, is generally large, and the propagation delay of these links is not negligible. Thus, ARQ may not work correctly, and a strong FEC method for correcting burst error is a good solution. In fact, the use of a low-density parity check (LDPC) code [2], turbo code [3], and low-density generator matrix (LDGM) code, which has erasure correcting ability for satellite laser communications, has been considered for error correction [4]. Error correction is performed effectively by these codes. However, their coding rate is relatively high, and the coding gains at a low rate are generally not high. Hence, an effective low-rate FEC for poor channel conditions is required in FSO.

Therefore, in this study, we focus on a rateless code, wherein the coding rate can be configured adaptively, and we propose a low-rate concatenated channel code based on the Reed–Solomon (RS) code and spinal code, which is one of the good rateless codes using soft decoding [5]. The proposed concatenated code is suitable for satellite laser communication channels when the total coding rate is low. In Section II, the downlink channel model of satellite-to-ground laser transmission is briefly introduced, The spinal code is described in Section III, and the proposed concatenation code based on the RS and spinal codes is explained in Section IV. The numerical results are presented in Section V, and conclusions are drawn in Section VI.

II. DOWNLINK SATELLITE-TO-GROUND CHANNEL MODEL

In satellite-to-ground laser communication, a burst degradation of received optical power occurs owing to the tracking error of the satellite and/or air turbulence. This causes serious degradation in communication quality. The probability density function (PDF) of received optical power in case of a weak disturbance due to air turbulence is given by a log-normal distribution [6]. When the received optical power is I and its average value is $< I >$, the PDF of I is given by

$$p_L(I) = \frac{1}{\sqrt{2\pi}I\sigma}\exp\left\{-\frac{\left[\ln\left(\frac{I}{<I>}\right)+\frac{1}{2}\sigma^2\right]^2}{2\sigma^2}\right\}, \qquad I>0 \tag{1}$$

where σ^2 is the distribution of I and is referred to as the scintillation index (SI), which is an index of air turbulence. When the SI is high, there is a considerable change in the received optical power. In case of a strong disturbance due to air turbulence, the PDF of I is given by the gamma-gamma distribution as follows: [7]

$$p_G(I) = \frac{2(\alpha\beta)^{\frac{\alpha+\beta}{2}}}{\Gamma(\alpha)\Gamma(\beta)} I^{\frac{\alpha+\beta}{2}-1} \times \mathrm{K}_{\alpha-\beta}\left(2\sqrt{\alpha\beta I}\right), \qquad I>0 \tag{2}$$

where $\Gamma()$ is the gamma function and $\mathrm{K_a}(b)$ is the modified Bessel function of the second kind, in which α and β are given as follows: [8]

$$\alpha = \left(\exp\left[\frac{0.49\sigma^2}{\left(1+1.11\sigma^{\frac{12}{5}}\right)^{\frac{7}{6}}}\right]-1\right)^{-1} \tag{3}$$

$$\beta = \left(\exp\left[\frac{0.51\sigma^2}{\left(1+0.69\sigma^{\frac{12}{5}}\right)^{\frac{7}{6}}}\right]-1\right)^{-1} \tag{4}$$

Here, the SI, i.e., σ^2, is given in terms of α and β as

$$\sigma^2 = \frac{1}{\alpha}+\frac{1}{\beta}+\frac{1}{\alpha\beta} \tag{5}$$

III. SPINAL CODES

As described in section I, ARQ is not effective for satellite laser communication owing to large propagation delay, whereas the adaptive control of the FEC coding rate is effective. Adaptive modulation and coding (AMC), where channel state information (CSI) is sent periodically from the receiver to the transmitter, and the transmitter changes the transmission rate accordingly, has been widely used in wireless communications [9]. However, the feedback delay for AMC is large in satellite communication, and an inappropriate modulation and coding set may get selected. Hence, an adaptive transmission with flexible coding rate and no feedback is required. Rateless codes have been proposed as a solution. Rateless codes can generate coded bits semi-permanently, and the code rate can be configured flexibly without feedback information. Spinal codes are a family of rateless codes that have strong correction ability. Thus, we considered applying a spinal code to satellite laser communication. The encoding and decoding schemes of the spinal code are reviewed briefly in the following paragraphs.

In spinal codes, a recursive hash function is used for encoding [10]. Fig. 1 shows the structure of a spinal encoder in a transmitter. Let the information bits to be encoded be represented as $\{0,1\}^N$. First, N information bits are divided per k bits and $N_k(=N/k)$ information sub-blocks are generated, each represented by $m_i(i=1,2,\dots,N_k)$. k is the number of sub-message bits. As shown in Fig. 1, m_i is encoded by the hash function h, and v bit outputs are obtained, labeled as S_i. The initial state of the encoder, S_0, is defined as $S_0=\{0\}^v$, and the i-th information sub-block m_i and the encoder state S_{i-1} are entered into the hash function. This operation is iterated N_k times and all S_i are generated. Next, v bits of S_i is divided per $2C$ bits, and the codewords are obtained, as shown in Fig. 2, where $x_{i,j}$ is the complex transmit symbol. Each value of $x_{i,j}$ consists of $2C$ bits, and S_i is divided into symbols labeled from $x_{i,1}$ to $x_{i,l}$. The former and latter C bits are allocated to the real and imaginary components of $x_{i,j}$, respectively. Here, the i and j in $x_{i,j}$ are referred to as depth and path, respectively. In the transmitter, i-th depth symbols ($i=1,2,\dots,N_k$) at the first path are transmitted sequentially; then, the symbols at the second path are transmitted. In addition, the decoding performance is improved by transmitting the last symbol $i=N_k$ redundantly as the tail symbol at each path [11].

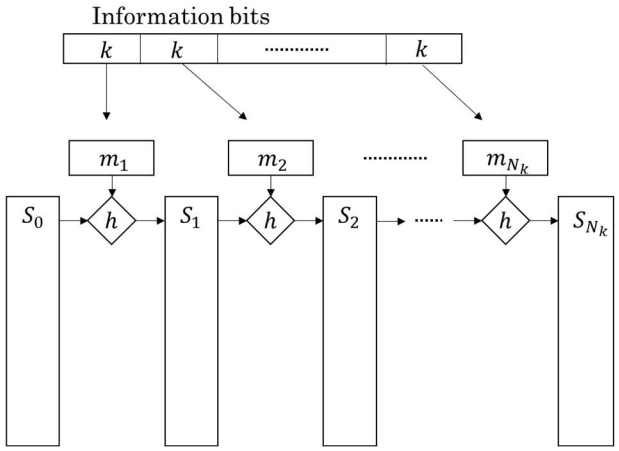

Fig. 1. Structure of spinal encoder.

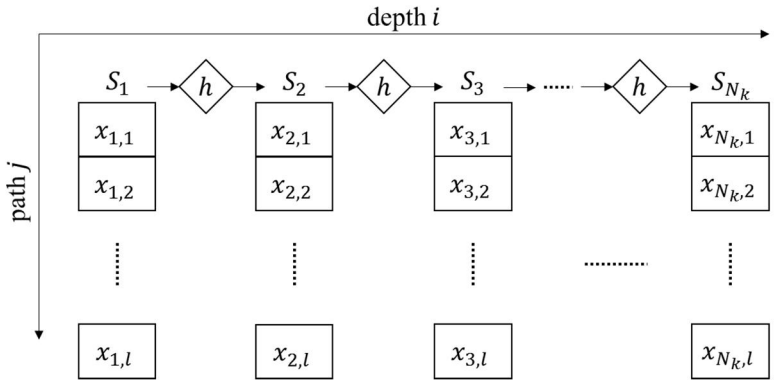

Fig. 2. Codeword and transmit symbol of spinal code.

For the decoding of spinal codes, bubble decoding is used; bubble decoding is a type of M-algorithm that reduces the complexity of maximum likelihood decoding [10]. Bubble decoding is a quasi-optimum decoding algorithm. It is assumed that the initial state S_0 and the hash function are known to the decoder. Then, because the number of input bits is k, there are 2^k branches from S_0 in the decoding search. At the decoding stage i, the branch metric for each branch from S_{i-1} is calculated as the squared Euclidean distance between the receive symbol and the corresponding replica symbol of the codeword. The branch metric $\gamma(i, \hat{x}(i))$ of the candidate symbol $\hat{x}(i)$ is given by

$$\gamma\big(i, \hat{x}(i)\big) = \sum_{j=1}^{l} ||r(i + (j-1)N_k) - \hat{x}(i + (j-1)N_k)||^2 \tag{6}$$

where $r(i)$ is the receive symbol and $||x||^2$ is the squared complex norm. The path metric Γ_i is defined as the summation of branch metrics until the stage i, which is given by

$$\Gamma_i(\hat{\mathbf{x}}_\mathbf{i}) = \sum_{j=1}^{i} \gamma(j, \hat{x}(j)) \tag{7}$$

where $\hat{\mathbf{x}}_\mathbf{i} = (\hat{x}(1), \hat{x}(2), \ldots, \hat{x}(i))$ is the decoding candidate sequence. During decoding, these metrics are calculated at stage N_k and the $\hat{x}_{N_k}$ having the minimum Γ_{N_k} is determined as the decoding result. However, in the spinal code, the number of branches from S_{i-1} is 2^k, and the total number of paths increases exponentially, which requires an exhaustive search. Therefore, bubble decoding adopts a parameter, beam width B, which is the number of survival paths at every stage. At stage S_i, B paths having the smallest metrics are kept as survival paths, and other paths are discarded. Thus, the exponential increase in decoding complexity is prevented. To increase the reliability of survival path selection, it has been proposed that the branch metrics of stage $(i + d -$

1) be taken into account when calculating the path metric at stage i, where d is a positive integer [10]. In this scheme, d should be determined appropriately because a high value of d leads to more calculation complexity.

IV. PROPOSED REED-SOLOMON AND SPINAL CONCATENATION CODE

Spinal codes utilize a hash function for encoding and decoding. When the number of input bits is higher than the number of output bits, the outputs from different information sub-blocks become identical in some cases. This is known as state collision. Because of state collision, spinal codes often have an error floor in the bit error rate (BER) performance, and the coding gain becomes saturated whenever the coding rate is lowered. Therefore, we applied the RS code, which is a strong code that is popular in satellite communications, as a concatenation code to the spinal code. We used a non-binary RS code and spinal code as the outer and inner codes, respectively. Fig. 3 shows the structure of the proposed encoder. First, the information bits are divided and undergo RS encoding. Next, the encoded bits are divided again and used as the input information sub-blocks for the hash function of the spinal code. Because the encoding and decoding of the spinal code are conducted by the information sub-block unit, the degree of the Galois field in RS coding becomes the same as the number of sub-blocks, which is effective in preventing extra error propagation between the two codes and obtaining a higher coding gain.

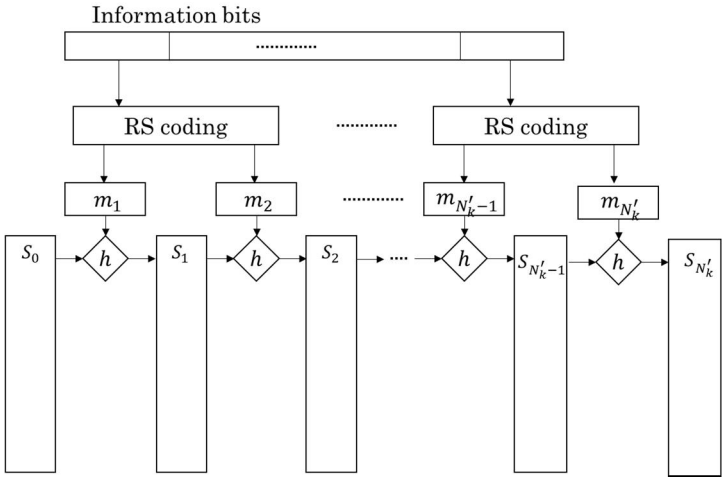

Fig. 3. Structure of proposed RS-spinal concatenation code.

V. NUMERICAL RESULTS

We compared the BER performance of the proposed scheme to that of a single spinal code in a downlink satellite laser channel in which air turbulence and additive white Gaussian noise (AWGN) were considered. Fig. 4 shows the block diagram of the proposed coding system, and the simulation conditions are listed in Table 1. First, 128 bit information was divided into four blocks. Next, it was transformed into a Galois field of GF(2^4), RS encoded, symbol interleaved, and transformed into binary four bits. Then, this bit stream was treated as the information sub-block for the hash function, and spinal encoded. We calculated the BER for different values of SI under the simulation conditions listed in Table 1. As shown in Fig. 5, when the SI is low, e.g., 0.1 or 0.2, the proposed concatenation code exhibits better performance than that of the single spinal code. However, for higher values of SI, the single spinal code exhibits better performance because the single spinal code with a low coding rate achieves better error correction. In RS coding, when the error symbols are more than the maximum number of error correctable symbols, the received codeword is output as is. Therefore, the performance of the proposed code degrades as the SI increases.

Next, the BER was calculated for the proposed concatenation code and the single spinal code for different values of the total coding rate, with values of SI ranging from 0.0 to 0.5. The results are shown in Figs. 6 and 7, where the coding rate of the RS code in the proposed scheme is fixed as 8/15 and the coding rate of the concatenated spinal code is changed. Other simulation parameters were the same as those listed in Table 1. It was shown that there are error floors in the single spinal code transmission because of state collision, as described in Section IV. In contrast, the BER of the proposed concatenation code decreased monotonically according to the decrease in coding rate. Thus, it was shown that the proposed scheme was effective in the low coding rate region.

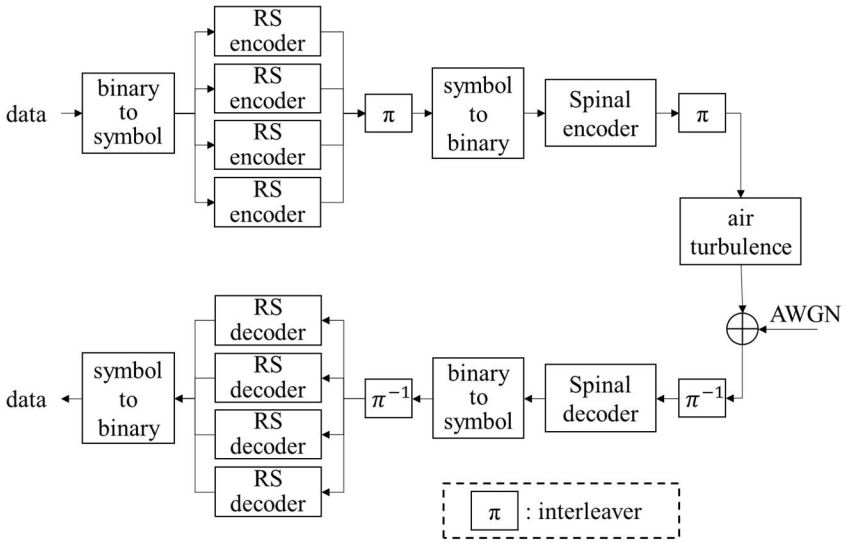

Fig. 4. System block diagram of proposed code.

VI. CONCLUSION

We proposed a low rate concatenation code—RS and spinal codes—for downlink satellite laser communication. Through numerical simulations, it was shown that the proposed scheme exhibited better performance than the single spinal code in the low coding rate region.

In future studies, adaptive coding rate transmission in the RS-spinal concatenation scheme will be considered.

Table 1. Simulation conditions.

code	RS-Spinal concatenation code	Spinal code
transmission bits	128	
coding rate R	(RS, Spinal) (8/15, 1/2) (8/15, 1/4)	1/4, 1/8
code length N	480, 960	512, 1024
modulation	BPSK ($C = 0.5$)	
channel	air fluctuation + AWGN	
air fluctuation-distribution	gamma-gamma	
E_b/N_0 [dB]	5	
transmission rate [Mbps]	1	
number of codewords W	10	
interleaver length	$N \times W$	
S parameter for interleaver	$\sqrt{N \cdot W}/4$	
number of bits per information sub-block	4	
hash function	Jenkins one-at-a-time	
output of hash function [bits]	32	
beam width B	16	
Galois field	GF(2^4)	-
RS coding information-symbols	8	-

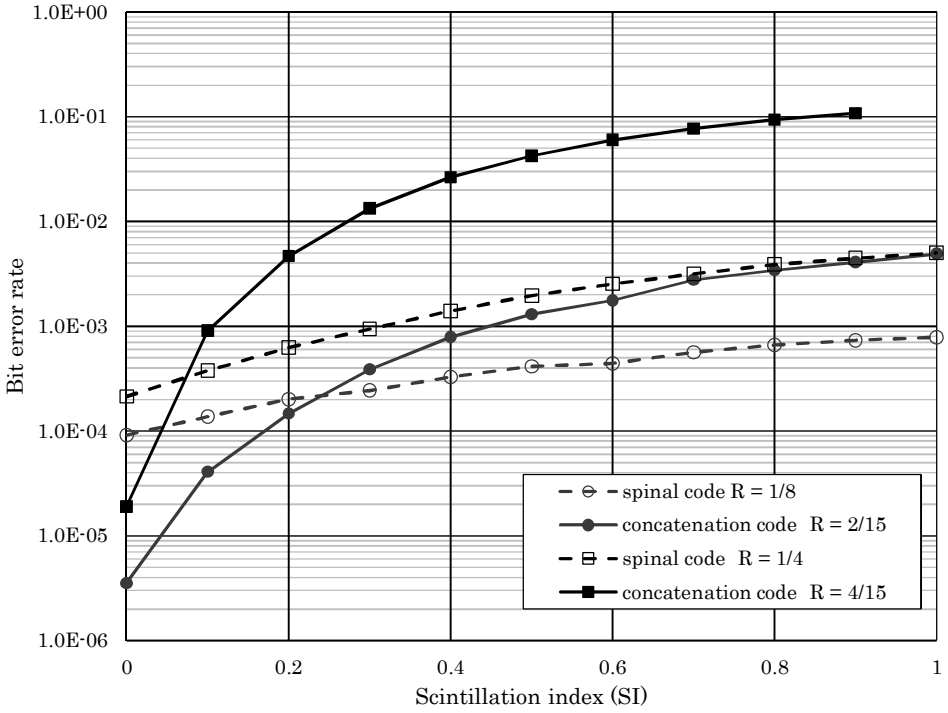

Fig. 5. Bit error rate versus scintillation index (SI).

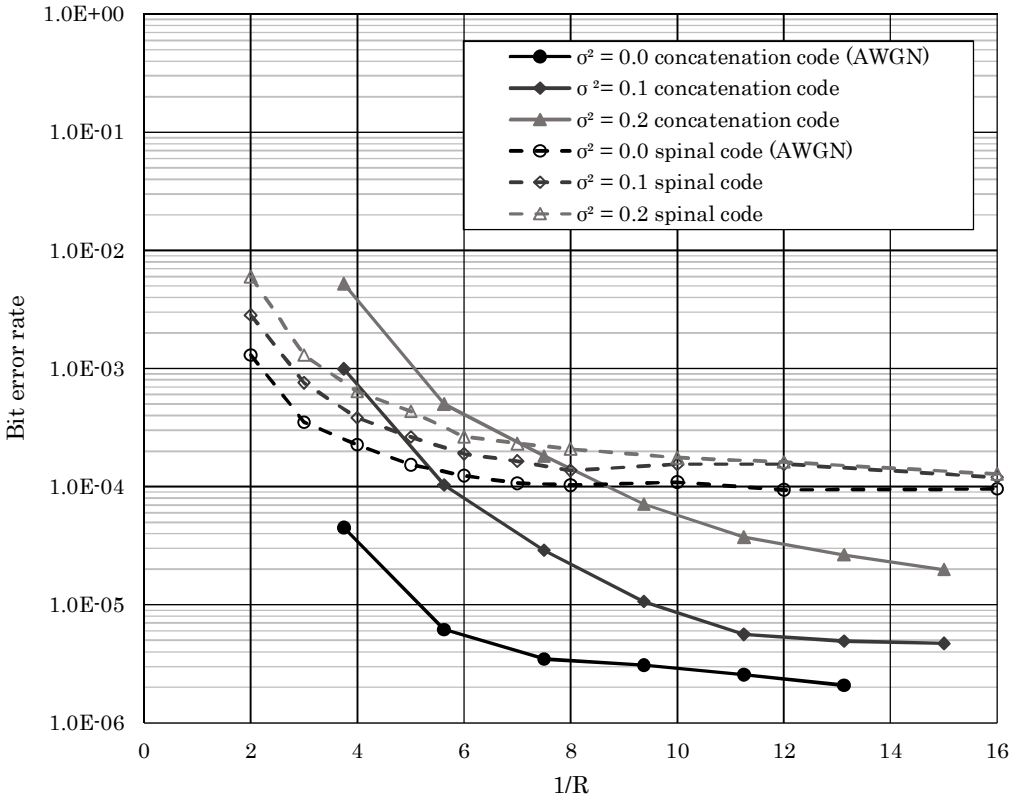

Fig. 6. Bit error rate versus coding rate (SI = 0.0 to 0.2).

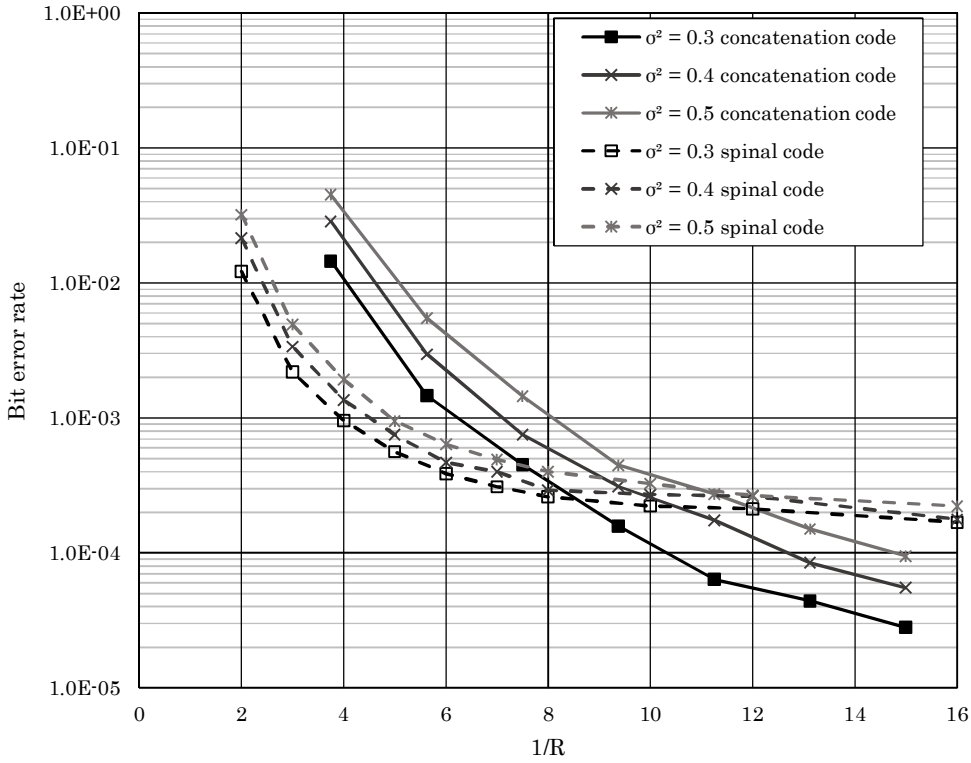

Fig. 7. Bit error rate versus coding rate (SI = 0.3 to 0.5).

REFERENCES

[1] "NICT NEWS," NICT, no. 456, Press 2016.

[2] R. G. Gallager, "Low Density Parity Check Codes," in Research Monograph series, Cambridge, MIT Press, 1963.

[3] C. Berrou, et.al, "Near Shannon Limit Error-Correcting Coding and Decoding: Turbo-Codes," Proc. IEEE Int'l Conf. on Commun.93, vol. 2, pp. 1064-1070, May. 1993.

[4] V. Roca, Z. Khallouf, and J. Laboure,"Design and Evaluation of a Low Density Generator Matrix (LGDM) Large Block FEC Codec," Fifth International Workshop on Networked Group Communication (NGC'03), Munich, Germany, Sept. 2003.

[5] J. Perry, H. Balakrishnan, and D. Shah, "Rateless Spinal Codes," Proc. ACM HotNets-X, Cambridge, MA, pp. 6:1-6:6, November 2011.

[6] L. C. Andrews, R. L. Phillips, and P. T. Yu, "Optical Scintillations and Fade Statistics for a Satellite-Communication System," Appl. Opt. vol. 34, no. 33, pp. 7742-7751(1995). Errata: 36(24), 6068(1997).

[7] L. C. Andrews, R. L. Phillips, Laser Beam Propagation Through Random Media (SPIE Optical Engineering Press, Bellingham, Wash., Second edition, 2005).

[8] N. Iwakiri, M. Toyoshima, "OOK Modulated Optical Satellite Communications System for CCSDS Standardization," 2015-j-16.

[9] A. Goldsmith, Wireless Communications, Cambridge University Press, 2015.

[10] J. Perry, P. Iannucci, K. E. Fleming, H. Balakrishnan, and D. Shah, "Spinal Codes," Proc. ACM SIGCOMM, Helsinki, Finland, August 2012.

[11] Y. Morishima, I. Oka, and S. Ata, "Threshold Algorithms for Decoding Spinal Codes," IEICE Tech. Rep., vol. 112, no. 460, IT2012-109, pp. 297-302, Mar. 2013.